Nonlinear polarization rotation and orthogonal polarization generation experienced in a single-beam configuration

N. Minkovski, G. I. Petrov, and S. M. Saltiel

Faculty of Physics, University of Sofia, 5 J. Bourchier Boulevard, BG-1164, Sofia, Bulgaria

O. Albert and J. Etchepare

Laboratoire d'Optique Appliquée, Unité Mixte de Recherche 7639, Centre National de la Recherche Scientifique, Ecole Nationale Supérieure de Techniques Avancées, Ecole Polytechnique, Centre de l'Yvette 91761, Palaiseau Cedex France

Received September 29, 2003; revised manuscript received April 7, 2004

Nonlinear polarization rotation and generation of a polarization component orthogonal to the input beam were observed along fourfold axes of YVO_4 and BaF_2 crystals. We demonstrate experimentally that in both crystals the angle of rotation is proportional, at low intensities, to the square of the product of the input intensity and the crystal length and is the result of simultaneous action of two third-order processes. This type of nonlinear polarization rotation is driven by the real part of the cubic susceptibility. The recorded energy exchange between the two orthogonal components can exceed 10%. It is to our knowledge the highest energy-conversion efficiency achieved in a single beam nonresonant $\chi^{(3)}$ interaction. A simple theoretical model is elaborated to describe the dependence of nonlinear polarization rotation and orthogonal polarization generation on the intensity of the input beam at both low- and high-intensity levels. It reveals the potential contributions from the real and the imaginary parts of the susceptibility tensor. Moreover, this kind of measurement is designed to permit the determination of the magnitude and the sign of the anisotropy of the real part of third-order nonlinearity in crystals with cubic or tetragonal symmetry on the basis of polarization-rotation measurements. The $\chi^{(3)}_{xxxx}$ component of the third-order susceptibility tensor and its anisotropy sign and amplitude value for BaF_2 and YVO_4 crystals are estimated and discussed.

OCIS codes: 190.0190, 190.4380, 190.4410, 190.4720, 230.5440, 160.4670.

1. INTRODUCTION

In general, light propagating through nonlinear crystals experiences nonlinear polarization rotation and induced ellipticity.[1,2] If we restrict ourselves to a nonlinear change of the polarization state in nongyrotropic crystals, we find in the literature[1–6] experimental and theoretical evidence that nonlinear polarization rotation is proportional to the imaginary part of $\chi^{(3)}$ anisotropy, whereas induced ellipticity is due to the real part. Although several theoretical analyses[7–9] have predicted that nonlinear polarization rotation can also exist in nondissipative cubic crystals, to our knowledge no experimental investigation has supported such a prediction. In a previous letter[10] we reported the existence of such a type of polarization rotation in YVO_4.

Here we investigate both theoretically and experimentally the effects of nonlinear rotation and orthogonal polarization generation that are due to $\mathrm{Re}[\chi^{(3)}]$ in a single-beam scheme, in a much bigger intensity range in both BaF_2 and YVO_4 crystals, demonstrating that in such experiments the achievement of 10% cross-polarized wave conversion and of polarization rotation of as much as 8° is possible.

This paper is organized as follows: In Section 2 we describe (i) the theoretical background of a process that generates a wave with an orthogonal polarization component, called a cross-polarized wave (XPW), and (ii) the effects of nonlinear rotation in cubic and tetragonal crystals based on $\mathrm{Re}[\chi^{(3)}]$. This is a further development of the model presented in Ref. 10, in which only small intensities were considered. Here we predict theoretically for the first time that rotational dependences will have a saw-toothed shape. In Section 3 we describe the experimental setup and the results of measurements of BaF_2 and YVO_4 crystals, namely, both the efficiency of generation of orthogonally polarized waves and the nonlinear polarization rotation. Estimation of the value of $\chi^{(3)}_{xxxx}$ and of the anisotropy of the third-order nonlinearity for YVO_4 is also given in the same section. The experiment confirmed the saw-toothlike form for the dependence on rotation of the XPW's efficiency and of the nonlinear rotation on the angle between the input polarization and the crystal axis.

2. THEORETICAL BACKGROUND

To describe the effects of polarization rotation and of the generation of orthogonal polarization components in cubic (and tetragonal) crystal with $4/mmm$ (and $m3m$) point group symmetry we consider, in the slowly varying envelope approximation, plane-wave propagation equations in which linearly polarized light enters a crystal along the crystal's fourfold axis [001]. Linear absorption is neglected, and the coordinate system is defined relative to

the direction of the input polarization. The equations that describe self-phase modulation of copolarized component A to the input wave and the orthogonal polarization component with amplitude B are written, on the condition that $|B| \ll |A|$ (i.e., neglecting depletion of wave A, self-phase modulation of wave B, and the possible effects of cross-phase modulation) as

$$\frac{dA}{dz} = -i\gamma_{\parallel}|A|^2A, \tag{1a}$$

$$\frac{dB}{dz} = -i\gamma_{\perp}|A|^2A, \tag{1b}$$

where $\gamma_{\parallel} = \gamma_0[1 - (\sigma/2)\sin^2(2\beta)]$ and $\gamma_{\perp} = -\gamma_0(\sigma/4)\sin(4\beta)$, with $\gamma_0 = (6\pi/8\lambda n)\chi^{(3)}_{xxxx}$ and $\sigma = [\chi^{(3)}_{xxxx} - 2\chi^{(3)}_{xyyx} - \chi^{(3)}_{xxyy}]/\chi^{(3)}_{xxxx}$ the anisotropy of the $\chi^{(3)}$ tensor.[1,11] Angle β is the angle between the input polarization and the [100] axis.

In general, coupling coefficients $\gamma_{\parallel}$ and $\gamma_{\perp}$ are complex quantities: $\gamma_{\parallel} = \gamma_{\parallel}' + i\gamma_{\parallel}''$ and $\gamma_{\perp} = \gamma_{\perp}' + i\gamma_{\perp}''$. The solutions of Eqs. (1) with initial conditions $B(0) = 0$ and $A(0) = A_0$ (A_0 is assumed to be real) are

$$A = A_0\exp(-i\gamma_{\parallel}A_0^2L), \tag{2a}$$

$$B = A_0(\gamma_{\perp}/\gamma_{\parallel})[\exp(-i\gamma_{\parallel}A_0^2L) - 1]. \tag{2b}$$

Using solutions (2), we consider separately the efficiency of XPW generation and the change of the polarization properties of the input wave A that are due to induced ellipticity and to nonlinear polarization rotation. Neglect of the depletion of wave A implies that solutions (2) and associated formulas can be applied only for XPW efficiencies not bigger than 10% and rotation angles smaller than 15°.

A. Efficiency of XPW Generation

From Eqs. (2) we find the following expression for the ratio of the two orthogonal polarization components (i.e., efficiency of XPW generation) at the output of the sample:

$$\eta = \left|\frac{B}{A}\right|^2 = |D|^2[1 + \exp(-2\Phi'') - 2\exp(-\Phi'')\cos(\Phi')], \tag{3}$$

where $\Phi' = \gamma_{\parallel}'A_0^2L$ is the nonlinear phase shift accumulated by wave A. Because it is a dimensionless quantity, Φ' will be used as a normalized intensity factor. For convenience we also introduce

$$\Phi'' = \gamma_{\parallel}''A_0^2L, \qquad D = \frac{\gamma_{\perp}}{\gamma_{\parallel}} = -\frac{1}{4}\left[\frac{\sigma\sin(4\beta)}{1 - (\sigma/2)\sin^2(2\beta)}\right]. \tag{4}$$

For purely real cubic nonlinearity and arbitrary input power,

$$\eta = 4\left(\frac{\gamma_{\perp}'}{\gamma_{\parallel}'}\right)^2\sin^2(\gamma_{\parallel}'A_0^2L/2). \tag{5}$$

We show in Fig. 1(a) the angular dependence of η for both high- and low-intensity excitation and opposite signs for anisotropy. At low level intensity (when $\Phi' \ll 1$), the angular dependence of η on β reduces to a pure $\sin^2(4\beta)$ law[5,10]:

$$\eta = (\gamma_{\perp}')^2A_0^4L^2. \tag{6}$$

For relatively high intensity (when $\Phi' \approx$ modulo π), the dependence of η on β deviates strongly from a $\sin^2(4\beta)$ law. This dependency measurement allows one to find the sign of anisotropy σ.

In Fig. 2 the dependence of the generation efficiency of the orthogonal component on power is shown. It turns out that, in a plane-wave approximation, the maximum

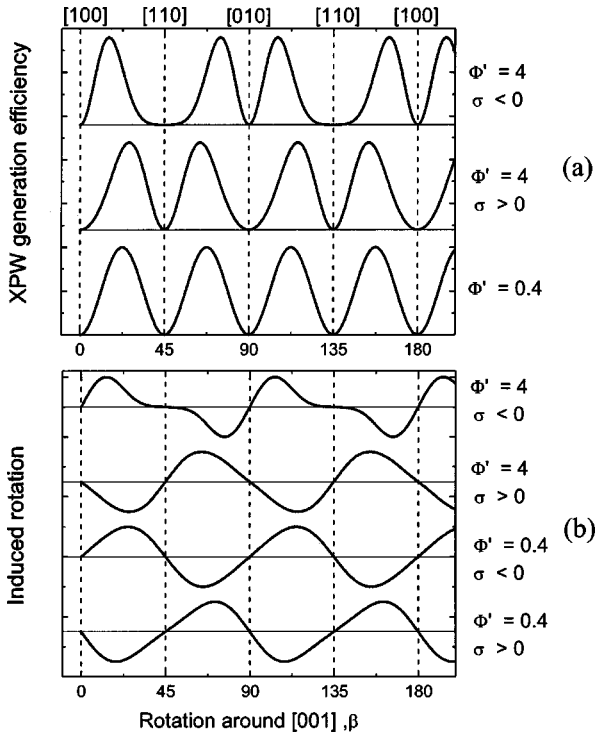

Fig. 1. (a) Dependence of the efficiency of XPW generation on crystal rotation and (b) dependence of induced nonlinear polarization on crystal rotation for two intensity levels, $\Phi' = 0.4$ and $\Phi' = 4$, and two values of anisotropy, $\sigma = 1$ and $\sigma = -1$. Each dashed line represents an angle for which the input polarization coincides with the indicated crystallographic axis.

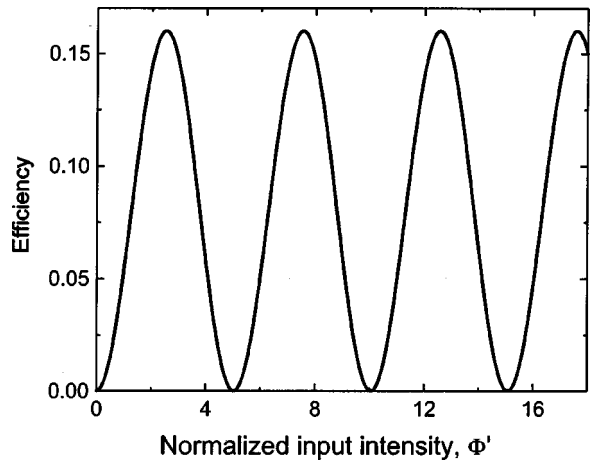

Fig. 2. Dependence of the efficiency of XPW generation on normalized input intensity Φ' for a nonlinear medium with predominantly real cubic nonlinearity. Angle $\beta = 22.5°$.

achievable conversion into a XPW depends only on the absolute value of anisotropy coefficient σ. Indeed, for normalized intensity $\Phi' = \pi$ and $\beta = \pi/8$,

$$\eta_{\max} = \left(\frac{2\sigma}{4 - \sigma}\right)^2. \tag{7}$$

For a nonlinear medium that has predominantly imaginary nonlinearity ($\gamma_\parallel' \ll \gamma_\parallel''$; $\gamma_\perp' \ll \gamma_\perp''$) the ratio of the intensities of the two orthogonal components is defined by

$$\eta = \left(\frac{\gamma_\perp''}{\gamma_\parallel''}\right)^2 [1 - \exp(-\gamma_\parallel'' A_0{}^2 L)]^2. \tag{8}$$

At low intensity levels, Eq. (8) is transformed into $\eta = (\gamma_\perp'')^2 A_0{}^4 L^2$. At these intensity levels the orthogonally polarized component is a direct result of the nonlinear rotation of the input wave with angle $\delta_0 = \gamma_\perp'' A_0{}^2 L$ (see, e.g., Ref. 3), and then the ratio of the intensities of the two polarization components will be $\sin^2(\delta_0) \approx \delta_0{}^2$, exactly as given by the low-intensity limit of Eq. (8). At high intensity ($\Phi'' \gg 1$) this ratio becomes constant; it does not depend either on the length of the medium or on the intensity: $\eta = (\gamma_\perp''/\gamma_\parallel'')^2$.

Huge differences between the behavior of the real and the imaginary components of the susceptibility tensor are in evidence. From these differences, one can conclude that the real or imaginary part of the third-order susceptibility is responsible for the effect of XPW generation.

B. Induced Ellipticity and Nonlinear Polarization Rotation

The fundamental beam going through the crystal changes its polarization properties: It experiences nonlinear rotation and induced changes in ellipticity.

Angle δ_0 of the main elliptical axis position and ellipticity angle ϵ at the output of the nonlinear medium can be found[12] with the help of the relations

$$\tan(2\delta_0) = 2\,\mathrm{Re}(\Gamma)/(1 - |\Gamma|^2), \tag{9}$$

$$\sin(2\epsilon) = 2\,\mathrm{Im}(\Gamma)/(1 + |\Gamma|^2), \tag{10}$$

where $\Gamma = B/A$ is the ratio of the complex amplitudes of the two orthogonal components.

For the general case of complex third-order nonlinearity, solutions for the induced rotation and ellipticity are

$$\tan(2\delta_0) = 2\,\frac{\mathrm{Re}(D) - [\mathrm{Re}(D)\cos\Phi' - \mathrm{Im}(D)\sin\Phi']\exp(-\Phi'')}{1 - \eta}, \tag{11}$$

$$\sin(2\epsilon) = 2\,\frac{\mathrm{Im}(D) - [\mathrm{Im}(D)\cos\Phi' + \mathrm{Re}(D)\sin\Phi']\exp(-\Phi'')}{1 + \eta}. \tag{12}$$

For predominantly real $\chi^{(3)}$ and arbitrary input intensity, Eqs. (11) and (12) are transformed into

$$\tan(2\delta_0) = 4\,\frac{(\gamma_\perp'/\gamma_\parallel')}{1 - \eta}\sin^2(\Phi'/2),$$

$$\sin(2\epsilon) = -2\,\frac{(\gamma_\perp'/\gamma_\parallel')}{1 + \eta}\sin\Phi'. \tag{13}$$

We recall that these expressions coincide, for small intensities ($\Phi' \ll \pi$), with those that were published in Ref. 10:

$$\tan(2\delta_0) \approx \gamma_\perp'\gamma_\parallel' A_0{}^4 L^2, \qquad \sin(2\epsilon) \approx -2\gamma_\perp' A_0{}^2 L. \tag{14}$$

The prime conclusion that can be deduced from Eqs. (14) is that measuring δ_0 or ϵ at a low intensity level leads to knowledge of the sign and the magnitude of anisotropy σ. Measurement at $\beta = +22.5°$ results in

$$\sigma = 4/(1 - 2\delta_0/\epsilon^2). \tag{15}$$

Furthermore, Eqs. (14) demonstrate that the nonlinear polarization rotation is proportional to the square of the cubic nonlinearity of the medium $\{\mathrm{Re}[\chi^{(3)}_{xxxx}]\mathrm{Re}[\chi^{(3)}_{xxxx}]\}$. This is a direct indication that this nonlinear polarization rotation is a result of two interlinked $\chi^{(3)}$ processes that are frequently called third-order cascaded process.[13–17] The two third-order interlinked processes are those described by Eqs. (1), namely, self-phase modulation of the input wave and the generation of a XPW wave by four-wave mixing. In the high-intensity regime ($\Phi' > 1$) the rotational patterns (β dependences) change drastically. Several examples of rotational patterns for predominantly real $\chi^{(3)}$ media are shown in Fig. 1(b).

For nonlinear media that have predominantly imaginary nonlinearities ($\gamma_\parallel' \ll \gamma_\parallel''$; $\gamma_\perp' \ll \gamma_\perp''$) the input linearly polarized wave does not lead to any ellipticity [$\sin(2\epsilon) = 0$], and the induced rotation becomes

$$\tan(2\delta_0) = 2\left(\frac{\gamma_\perp''}{\gamma_\parallel''}\right)\frac{[1 - \exp(-\gamma_\parallel'' A_0{}^2 L)]}{1 - \eta}. \tag{16}$$

At low intensity, Eq. (16) is transformed to the known expression[3]

$$\tan(2\delta_0) = 2\gamma_\perp'' A_0{}^2 L. \tag{17}$$

Thus, comparing Eqs. (14) and (17), we can see that the induced polarization also strongly depends on the characteristics of the nonlinearity: the dependence is quadratic for pure real $\chi^{(3)}$ and linear when the rotation is due to the imaginary part of $\chi^{(3)}$.

3. EXPERIMENT

The experiment was performed with a single beam that propagates along the z axes of [001]-cut yttrium vanadate (YVO_4; $4/mmm$ point group symmetry) and barium fluoride (BaF_2; $m3m$ point group symmetry). The z axes of these two crystals have fourfold symmetry, and they have no linear optical activity. Two samples of BaF_2 were available from different producers. The length of each sample was 0.9 mm. The setup consisted of a colliding-pulse mode-locked dye laser (maximum energy, 60 μJ; duration, 100 fs; frequency, 10 Hz; wavelength, 620 nm), an input polarizer, and an output analyzer. The laser beam

was focused onto the sample with a 50-cm focal-length lens. The signals from two photodiodes that measure input and output energies were connected to a computer for signal averaging and processing. We performed measurements of the signal coming out from the sample sandwiched between the polarizer and the analyzer as a function of β, the angle of the input polarization plane with respect to the [100] axis of the crystal. For exactly crossed polarizer and analyzer (setup I), the signal measures the dependence of the XPW-generation efficiency on β.[18] To study the output polarization state (induced ellipticity and nonlinear polarization rotation) we performed extinction curve measurements by introducing small angular deviations δ from the exact crossed position between the two polarizers (setup II). The two-photon absorption and its anisotropy were estimated by measurement of the sample transmission for the same ensemble of β values.

The results of the measurements of the efficiency of XPW generation by use of setup I at different levels of input intensity are shown in Fig. 3. Maxima of the efficiency for low input energy when $\gamma_{\parallel}' A_0^2 L \ll 1$ [Fig. 3(a)] appear at angular positions $22.5° + j(\pi/4)$ (j an integer), consistent with Ref. 5 and the theory described above. For high input energy the angular distance between two neighboring maxima is smaller or bigger than 45°, depending on the orientation of the sample. As can be seen from Fig. 3, the two neighboring maxima close to the [010] axis appear at an angular distance smaller than 45° for BaF_2 [Fig. 3(c)], whereas for YVO_4 this distance is bigger than 45° [Fig. 3(b)]. From this fact we conclude that values of anisotropy σ of the $\chi^{(3)}$ tensor for the two crystals investigated are opposite in sign.

Using setup I, we also measured efficiency as a function of input pulse energy of XPW generation for the two samples. At fixed energy the XPW signal from the YVO_4 sample was more than an order of magnitude stronger than the signal from BaF_2. As can be seen from Fig. 4, the dependence of efficiency on the energy of the input pulse clearly follows a quadratic slope as predicted by the theoretical analysis presented in Section 2 [Eq. (5)]. At the highest energy levels, saturation is observed; it is connected with the periodical character of the energy exchange between the two orthogonal components. The different slopes in the initial parts of the curves are a consequence of linear depolarization that most probably is due to residual stress[5] and to intrinsic birefringence.[19] As can be seen from Fig. 4, two different samples produce a big difference in linear depolarization that we can explain as being due to the different levels of residual stress.

The highest recorded energy exchange between the two orthogonal components exceeds 10% and according to our knowledge is the highest efficiency achieved with single-beam nonresonant $\chi^{(3)}$ interaction in a single centrosymmetric medium. The reason for the good XPW-generation efficiency is that it is characterized by an automatically perfect and simultaneous phase- and group-velocity match along the z axis. The closest result to our measurements is reported in Ref. 20, where 8% XPW generation was measured in ZnSe. At the same time we have to note that recently several experimental papers reported single quadratic crystal third-harmonic

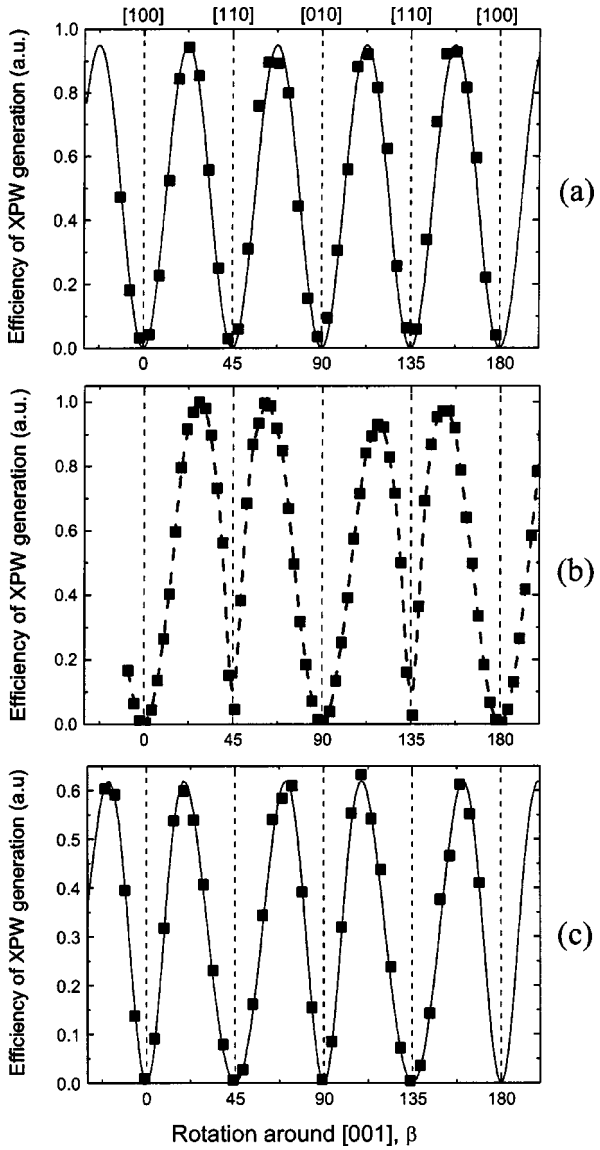

Fig. 3. Experimentally measured evolution of the signal, through crossed polarizer and analyzer, as a function of a sample's rotation about its [001] axis for two levels of intensity. Dashed lines, as in Fig. 1, correspond to input polarization parallel to the [100], [110], or [010] axis. Solid curves in (a) and (c) were plotted with theoretical formulas obtained in Subsection 2.A. The dotted curve in (b) is a guide for the eye. (a) YVO_4, $\Phi' \ll 1$ ($W_{in} = 0.7\ \mu J$); (b) YVO_4, $\Phi' > 1$ ($W_{in} = 11.5\ \mu J$); (c) BaF_2, $\Phi' > 1$ ($W_{in} = 39\ \mu J$).

generation in which the efficiency of third-harmonic generation is greater than 20%.[21–23] In the last case, however, the process is based on cascaded effective cubic nonlinearity proportional to the product $[\chi^{(2)}\chi^{(2)}]$ (for a review of these papers, Ref. 24).

To estimate the $\chi^{(3)}_{xxxx}$ component from YVO_4 we used the following relation, deduced from Eq. (6), that is suitable for measurement of relative susceptibility at power levels far from saturation:

$$\chi^{(3)}_{xxxx}(YVO_4) = \frac{n_{YVO_4}}{n_{BaF_2}} \sqrt{\frac{\eta_{YVO_4}}{\eta_{BaF_2}}} \frac{L_{BaF_2}}{L_{YVO_4}} \frac{\sigma_{BaF_2}}{\partial_{YVO_4}} \chi^{(3)}_{xxxx}(BaF_2). \tag{18}$$

Using the average value of several measurements, $\eta_{YVO_4}/\eta_{BaF_2} = 26 \pm 10\%$, we obtained $\chi^{(3)}_{xxxx}(YVO_4) = (8.2 \pm 2.1)\chi^{(3)}_{xxxx}(BaF_2)$. With the help of published data for $\chi^{(3)}_{xxxx}(BaF_2)$ the absolute value of $\chi^{(3)}_{xxxx}(YVO_4)$ can be calculated. For example, taking the data published in Ref. 25, $\chi^{(3)}_{xxxx}(BaF_2) = 1.59 \times 10^{-22}\,m^2/V^2$, we obtained the value $\chi^{(3)}_{xxxx}(YVO_4) = +13.0 \times 10^{-22}\,m^2/V^2$. The plus was found from the z-scan test. The badly defined spatial distribution quality of the beam did not allow us to perform absolute measurements.

By recording the extinction curves with setup II (as we described in Ref. 10) we were able to obtain the β and power dependences for the nonlinear rotation and the induced ellipticity. In Fig. 5 the dependence of β on rotation measured with both samples at energy levels below the region where saturation begins is shown. It can be clearly seen from Fig. 5 that the angular position of the extremum of the nonlinear rotation does not coincide with the angular position of the maximum of the XPW generation at the same power levels [see, for comparison, Fig. 3(a)]. Moreover, from the fit with the theoretical model for δ_0 the magnitude and the sign of the anisotropy σ can be estimated; by way of illustration, the two experimental curves in Fig. 5 are compared with the theoretical predictions calculated according Eq. (14) with $\sigma = -1.2$ for the BaF_2 sample and with $\sigma = +1$ for YVO_4. Similar values were deduced from the dependence on power of the nonlinear rotation and induced ellipticity. The variations of the measured nonlinear polarization rotation and induced ellipticity with increasing input laser energy for the YVO_4 sample are shown in Fig. 6. From the initial nonsaturated parts of the curves in Fig. 6 and from the same dependences for the BaF_2 sample and using Eq. (15), we obtained $\sigma = +1.0 \pm 10\%$ for YVO_4 and $\sigma = -1.15 \pm 10\%$ for BaF_2. These values are in excellent agreement with the values obtained from Fig. 5; also, the value for BaF_2 is in good agreement with the published value, $\sigma = -1.08 \pm 0.10$.[25]

We have described a new, simple single-beam method for measuring anisotropy σ of the $\chi^{(3)}$ tensor in cubic and tetragonal crystals, a procedure that can be used as an alternative to the known z-scan scheme.[26] The positive value for σ in YVO_4 is close to the value that has been measured for CdTe and GaAs at wavelengths that correspond to fundamental photon energy above half of the bandgap,[27] where a resonance change of the sign of σ is expected. We calculated that our fundamental wavelength (620 nm) corresponds to $\hbar\omega/E_g \approx 0.64$ for YVO_4 and to $\hbar\omega/E_g \approx 0.22$ for BaF_2.

The fact that nonlinear rotation δ_0 in the initial part of Fig. 6 shows a quadratic dependence on input intensity demonstrates that the effect of nonlinear rotation is due to the real part of $\chi^{(3)}$, in accordance with Eqs. (14). If the nonlinear rotation were due to the imaginary part of $\chi^{(3)}$, then the dependence of the nonlinear rotation on intensity would be linear, as one can see from Eq. (17). Independently, the separate measurement of the anisotropy of $\mathrm{Im}[\chi^{(3)}]$ at $W_{in} = 2\ \mu J$ (Ref. 10) ensures that the nonlinear rotation that is due to the imaginary part of $\chi^{(3)}$ is an order of magnitude less, a fact that confirms that the main contributor to the observed nonlinear rotation and XPW generation is $\mathrm{Re}[\chi^{(3)}]$. Finally, we point out that

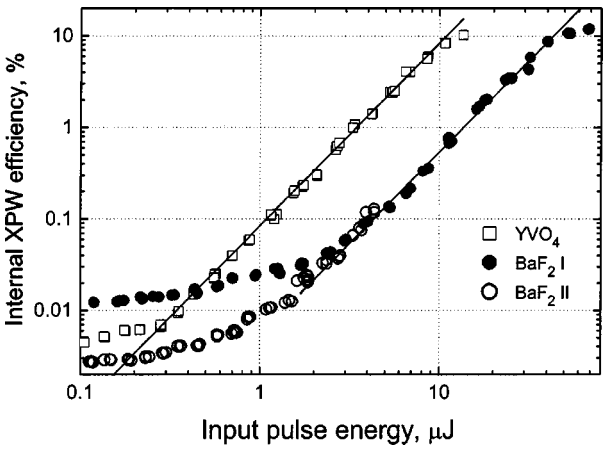

Fig. 4. Variation of the efficiency of XPW generation measured at $\beta = 22.5°$ as a function of input laser energy. Solid curves are quadratic fits.

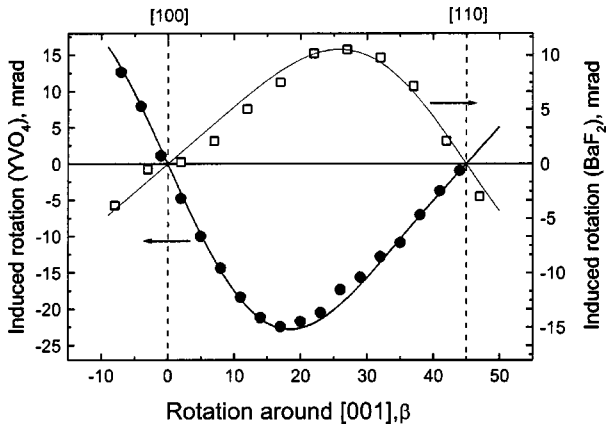

Fig. 5. Experimentally measured nonlinear polarization rotation as a function of a sample's rotation about its [001] axis for $\Phi' \leq 1$ for YVO_4 ($W_{in} = 4\ \mu J$) and BaF_2 ($W_{in} = 15\ \mu J$). The dashed lines have the same meaning as in Figs. 1 and 3. Solid curves were plotted with theoretical formulas obtained in Subsection 2.A by use of $\sigma = -1.2$ for the BaF_2 curve and $\sigma = 1$ for the YVO_4 curve.

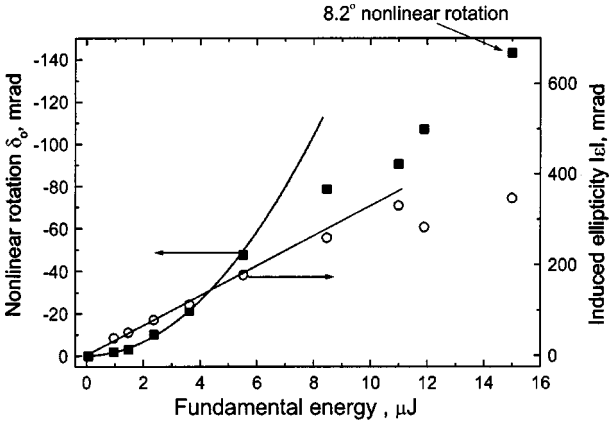

Fig. 6. Variation of the measured nonlinear polarization rotation and induced ellipticity as a function of input laser energy as obtained with the YVO_4 sample. $\beta = 22.5°$. Solid curves are quadratic and linear fits.

nonlinear rotations exceeding 8° (as illustrated in Fig. 6) have been measured in an YVO_4 sample.

4. CONCLUSIONS

We have reported in detail our theoretical and experimental investigation of the nonlinear optical self-interaction effects that occur when an intense laser light wave propagates along the fourfold axes of centrosymmetric crystals. YVO_4 and other cubic and tetragonal crystals are used as host crystals for active elements for solid-state lasers.[28] BaF_2 is one of the best materials for UV optics systems. Knowledge of the effects described above is therefore important for avoiding unwanted depolarization in optical elements made from these materials. Knowledge of the third-order nonlinearity in these crystals is also essential for prediction of potential Kerr-lens mode locking or for avoiding unwanted phase modulation effects. The polarization-sensitive effects that we describe can facilitate measuring the magnitude and the sign of the cubic nonlinearity tensor's components and its anisotropy in crystals. The attractive aspect of the proposed $\chi^{(3)}$ measurement method lies in the fact that it is a single-beam technique, with pumping and recording at the same wavelength.

ACKNOWLEDGMENTS

The project described here was performed within "Access to Research Infrastructure" contract (LIMANS III, CT-1999-00086). N. Minkovski and S. M. Saltiel thank the Laboratoire d'Optique Appliquée, Ecole Polytechnique, for hospitality and support during their stay and also the Bulgarian Ministry of Science and Education for partial support through Science Fund grant 1201/2002.

S. M. Saltiel's e-mail address is saltiel@phys.uni-sofia.bg.

REFERENCES

1. W. A. Schroeder, D. S. McCallum, D. R. Harken, M. D. Dvorak, D. R. Andersen, A. L. Smirl, and B. S. Wherrett, "Intrinsic and induced anisotropy of nonlinear absorption and refraction in zinc blende semiconductors," J. Opt. Soc. Am. B **12**, 401–415 (1995).
2. Yu. P. Svirko and N. I. Zheludev, *Polarization of Light in Nonlinear Optics* (Wiley, New York, 1998).
3. M. G. Dubenskaya, R. S. Zadoyan, and N. I. Zheludev, "Nonlinear polarization spectroscopy in GaAs crystals: one- and two-photon resonances, excitonic effects, and the saturation of nonlinear susceptibilities," J. Opt. Soc. Am. B **2**, 1174–1178 (1985).
4. A. I. Kovrigin, D. V. Yakovlev, B. V. Zhdanov, and N. I. Zheludev, "Self-induced optical activity in crystals," Opt. Commun. **35**, 92–95 (1980).
5. R. S. Zadoyan, N. I. Zheludev, and L. B. Meysner, "Nonlinear polarization spectroscopy of ions interaction potential in alkali halide crystals," Solid State Commun. **55**, 713–715 (1985).
6. A. D. Petrenko and N. I. Zheludev, "Physical mechanisms of nonlinear optical activity in crystals," Opt. Acta **31**, 1177–1184 (1984).
7. M. I. Dykman and G. G. Tarasov, "Self-induced change in the polarization of electromagnetic waves in cubic crystals," Fiz. Tverd. Tela (Leningrad) **24**, 2396–2402 (1982) [Sov. Phys. Solid State **24**, 1361–1364 (1982)].
8. D. C. Hutchings, "Nonlinear-optical activity owing to anisotropy of ultrafast nonlinear refraction in cubic materials," Opt. Lett. **20**, 1607–1609 (1995).
9. D. C. Hutchings, J. S. Aitchison, and J. M. Arnold, "Nonlinear refractive coupling and vector solitons in anisotropic cubic media," J. Opt. Soc. Am. B **14**, 869–879 (1997).
10. N. Minkovski, S. M. Saltiel, G. I. Petrov, O. Albert, and J. Etchepare, "Polarization rotation induced by cascaded third-order processes," Opt. Lett. **27**, 2025–2027 (2002).
11. M. D. Dvorak, W. A. Schroeder, D. R. Andersen, A. L. Smirl, and B. S. Wherrett, "Measurement of the anisotropy of two photon absorption coefficient in zincblende semiconductors," IEEE J. Quantum Electron. **30**, 256–267 (1994).
12. R. M. Azzam and N. M. Bashara, *Ellipsometry and Polarized Light* (North-Holland, Amsterdam, 1977).
13. S. Akhmanov, V. Martinov, S. Saltiel, and V. Tunkin, "Nonresonant six photon process in calcite crystal," Pis'ma Zh. Eksp. Teor. Fiz. **22**, 143–147 (1975) [JETP Lett. **22**, 65–67 (1975)].
14. S. Saltiel, S. Tanev, and A. D. Boardman, "High order nonlinear phase shift due to cascaded third order processes," Opt. Lett. **22**, 148–150 (1997).
15. V. Astinov, K. J. Kubarych, C. J. Milne, and R. J. D. Miller, "Diffractive optics implementation of six-wave mixing," Opt. Lett. **25**, 853–855 (2000).
16. L. Misoguti, S. Backus, C. G. Durfee, R. Bartels, M. M. Murnane, and H. C. Kapteyn, "Generation of broadband VUV light using third-order cascaded processes," Phys. Rev. Lett. **87**, 013601 (2001).
17. C. G. Durfee, L. Misoguti, S. Backus, H. C. Kapteyn, and M. M. Murnane, "Phase matching in cascaded third-order processes," J. Opt. Soc. Am. B **19**, 822–831 (2002).
18. G. I. Petrov, O. Albert, J. Etchepare, and S. M. Saltiel, "Cross-polarized wave generation by effective cubic nonlinear optical interaction," Opt. Lett. **26**, 355–357 (2001).
19. J. H. Burnett, Z. H. Levine, and E. L. Shirley, "Intrinsic birefringence in calcium fluoride and barium fluoride," Phys. Rev. B **64**, 241102 (2001).
20. M. Dabbicco, A. M. Fox, G. von Plessen, and J. F. Ryan, "Role of $\chi^{(3)}$ anisotropy in the generation of squeezed light in semiconductors," Phys. Rev. B **53**, 4479–4487 (1996).
21. C. Zhang, H. Wei, Y. Y. Zhu, H. T. Wang, S. N. Zhu, and N. B. Ming, "Third-harmonic generation in a general two-component quasi-periodic optical superlattice," Opt. Lett. **26**, 899–901 (2001).
22. Y. Q. Qin, Y. Y. Zhu, S. N. Zhu, and N. B. Ming, "Quasi-phase-matched harmonic generation through coupled parametric processes in a quasiperiodic optical superlattice," J. Appl. Phys. **84**, 6911–6916 (1998).
23. S. Zhu, Y. Y. Zhu, and N. B. Ming, "Quasi-phase-matched third-harmonic generation in a quasiperiodic optical superlattice," Science **278**, 843–846 (1997).
24. S. M. Saltiel, A. A. Sukhorukov, and Y. S. Kivshar, "Multistep parametric processes in nonlinear optics," in *Progress in Optics Vol. 47*, E. Wolf, ed. (Elsevier, Amsterdam, to be published).
25. R. DeSalvo, M. Sheik-Bahae, A. A. Said, D. J. Hagan, and E. W. Van Stryland, "Z-scan measurements of the anisotropy of nonlinear refraction and absorption in crystals," Opt. Lett. **18**, 194–196 (1993).
26. M. Sheik-Bahae, A. A. Said, T. H. Wei, D. J. Hagan, and E. W. Van Stryland, "Sensitive measurement of optical nonlinearities using a single beam," IEEE J. Quantum Electron. **26**, 760–769 (1990).
27. T. D. Krauss, J. K. Ranka, F. W. Wise, and A. L. Gaeta, "Measurements of the tensor properties of third-order nonlinearities in wide-gap semiconductors," Opt. Lett. **20**, 1110–1112 (1995).
28. W. Koechner, *Solid-State Laser Engineering*, 5th ed., Vol. 1 of Springer Series in Optical Sciences (Springer-Verlag, Berlin, 1999).